Journal of Neurochemistry

JOURNAL OF NEUROCHEMISTRY | 2015 | 134 | 538–550 doi: 10.1111/jnc.13149

ORIGINAL ARTICLE

Metabolic clues to salubrious longevity in the brain of the longest-lived rodent: the naked mole-rat

Judy C. Triplett,* Aaron Swomley,* Jessime Kirk,* Katilyn Lewis,†,‡ Miranda Orr,†,§ Karl Rodriguez,†,§ Jian Cai,¶ Jon B. Klein,¶ Rochelle Buffenstein†,§ and D. Allan Butterfield*,**

*Department of Chemistry, University of Kentucky, Lexington, Kentucky, USA

†Sam and Ann Barsop Institute for Longevity and Aging Studies, University of Texas Health Science Center, San Antonio, Texas, USA

‡Department of Cellular and Structural Biology, University of Texas Health Science Center, San Antonio, Texas, USA

§Department of Physiology, University of Texas Health Science Center, San Antonio, Texas, USA

¶Department of Nephrology and Proteomics Center, University of Louisville, Louisville, Kentucky, USA

**Sanders-Brown Center on Aging, University of Kentucky, Lexington, Kentucky, USA

Abstract

Naked mole-rats (NMRs) are the oldest-living rodent species. Living underground in a thermally stable ecological niche, NMRs have evolved certain exceptional traits, resulting in sustained health spans, negligible cognitive decline, and a pronounced resistance to age-related disease. Uncovering insights into mechanisms underlying these extraordinary traits involved in successful aging may conceivably provide crucial clues to extend the human life span and health span. One of the most fundamental processes inside the cell is the production of ATP, which is an essential fuel in driving all other energy-requiring cellular activities. Not surprisingly, a prominent hallmark in age-related diseases, such as neurodegeneration and cancer, is the impairment and dysregulation of metabolic pathways. Using a two-dimensional polyacrylamide gel electrophoresis proteomics approach, alterations in expression and phosphorylation levels of metabolic proteins in the brains of NMRs, aged 2–24 years, were evaluated in an age-dependent manner. We identified 13 proteins with altered levels and/or phosphorylation states that play key roles in various metabolic pathways including glycolysis, β-oxidation, the malate-aspartate shuttle, the Tricarboxylic Acid Cycle (TCA) cycle, the electron transport chain, NADPH production, as well as the production of glutamate. New insights into potential pathways involved in metabolic aspects of successful aging have been obtained by the identification of key proteins through which the NMR brain responds and adapts to the aging process and how the NMR brain adapted to resist age-related degeneration.

Keywords: aging, health span, metabolism, naked mole-rats, phosphoproteomics, proteomics.

J. Neurochem. (2015) **134**, 538–550.

Most aging research focuses on investigating a few well-characterized short-lived species including *Caenorhabditis elegans*, *Drosophila melanogaster, Rattus norvegicus,* and *Mus musculus* (Finch and Austad 2001). While models with such short life spans provide the ability to perform experiments rapidly, restraining biomedical research to very few models of aging or longevity may limit novel discoveries and scientific progression. Not surprisingly, there is a growing call for new models that may better mimic human aging and provide better translational predictability (Buffenstein *et al.* 2014). Since humans are a long-living species on the basis of their body size (Hulbert *et al.* 2007), it is hypothesized that species with naturally longer lives may yield better insights into diseases that afflict humans later in life than do short-lived models that commonly die before age-related diseases manifest. Such species likely also have evolved mechanisms

Received February 19, 2015; revised manuscript received April 13, 2015; accepted April 23, 2015.

Address correspondence and reprint requests to D. Allan Butterfield, Department of Chemistry and Sanders-Brown Center on Aging, University of Kentucky, Lexington, KY 40506-0055, USA. E-mail: dabcns@uky.edu; Rochelle Buffenstein, Barshop Institute for Aging and Longevity Studies, San Antonio, TX 78245, USA. E-mail: buffenstein@uthscsa.edu

Abbreviations used: BACH, brain acyl-CoA hydrolase; IEF, isoelectric focusing; LDH, lactate dehydrogenase; NMRs, naked mole-rats.

that allow for extended healthy life spans, in contrast to those that do not, and as such provide more precise models for human aging (Lewis *et al.* 2012). Unlike most other rodents that live relatively short lives in absolute terms (as little as 2–3 months in the wild; 2–5 years in captivity), naked mole-rats (NMRs) live to exceedingly advanced ages (4–17 years in the wild and up to 30+ years in captivity), unrivaled by any other rodent species (Bobeck 1969; David and Jarvis 1985; Buffenstein 2008; Edrey *et al.* 2011). Perhaps even more extraordinary, NMRs exhibit a prolonged health span, seemingly resistant to age-related deterioration well into old age (Buffenstein 2008; Edrey *et al.* 2011; Grimes *et al.* 2014). Insights into mechanisms facilitating sustained physiology and metabolism in NMRs may have therapeutic implications for human aging and age-associated diseases.

NMRs are naturally found in the arid and semi-arid regions of the horn of Africa (Kenya, Ethiopia and Somalia). Here, they lead an exclusive subterranean existence, living in sealed burrows in large eusocial colonies of up to 300 individuals with a strict division of labor culminating in the presence of only one breeding female and 2–4 breeding males (Jarvis 1981). This extreme environment coupled with their eusocial life style has led to the evolution of several adaptive traits including tolerance of variable oxygen and nutrient availability and concomitant metabolic effects (Buffenstein and Yahav 1991a,b; Larson and Park 2009).

NMRs present a number of unique phenotypes that may contribute to their unusually long lives. NMRs maintain a low basal metabolic rate throughout their lives (O'Connor *et al.* 2002). This is accompanied by low heart rates, decreased cardiac output, and low fasting blood glucose levels (Ables *et al.* 2014; Grimes *et al.* 2014). Nevertheless, glucose tolerance tests reveal that a large dose of glucose will cause a prolonged blood glucose elevation, indicative of insulin insensitivity (Kramer and Buffenstein 2004). This insensitivity is characteristic of induced-diabetic animal models, yet healthy NMRs show no other signs of diabetic pathology (Dumm *et al.* 1995; Tokuyama *et al.* 1995; Kramer and Buffenstein 2004). Rather, animals appear to be extremely sensitive to insulin administration. Unlike mice treated in an identical manner, glucose levels in blood not only precipitously drop following treatment with human insulin but remain at these low levels for an extended period (Dumm *et al.* 1995; Tokuyama *et al.* 1995; Kramer and Buffenstein 2004). These findings suggest that in their normal daily lives they are extremely sensitive to insulin signaling. Novel and tightly regulated glucose management may play a critical role in life span extension as it has been shown that genetic control of insulin signaling through the insulin/insulin-like growth factor signaling pathway may significantly expand the life span of an organism (Guarente and Kenyon 2000).

In this study, we explored not only the age-dependence of levels of brain proteins involved in energy metabolism, but also their global phosphorylation status as a means of gathering insights into the active proteome of NMRs during their life and development. The brain, in particular, is an essential organ on which to study, as cerebral insulin signaling is crucial in maintaining energy and glucose homeostasis, arguably key regulators of longevity and aging. Dysregulation of these pathways is associated with neurodegenerative diseases and metabolic syndromes leading to shortened life spans and diminished quality of life (Butterfield *et al.* 2014).

By evaluating the NMR proteome and phosphoproteome, the results obtained have yielded a number of insights into the salubrious aging process of NMR with regard to glucose utilization, proteostasis networks, signaling pathways, neuronal plasticity, and neuronal structure. A large number of brain proteins altered in aging have been identified, too many to be efficiently presented and discussed in a single manuscript. Accordingly, to facilitate the discussion of the implications of altered protein expression and phosphorylation and how they relate to the unusually long and healthy life spans of NMRs, we approached this effort by use of functional class of identified proteins. Here, we present the results related to metabolism.

Materials and methods

Materials

The chemicals used in these studies were purchased from Sigma-Aldrich (St. Louis, MO, USA) unless otherwise noted. Criterion precast polyacrylamide gels, ReadyStrip IPG strips (pH 3–10), TGS and MOPS electrophoresis running buffers, 0.2 nm nitrocellulose membrane, Precision Plus Protein All Blue Standards, Sypro Ruby Protein Stain, urea, biolytes, mineral oil, dithiothreitol (DTT), and iodoacetamide were obtained from Bio-Rad (Hercules, CA, USA). Modified trypsin solution was purchased from Promega (Madison, WI, USA). C_{18} ZipTips, and Re-Blot Plus Strong stripping solution were purchased from Millipore (Billerica, MA, USA). Pro-Q Diamond phosphoprotein stain, and anti-phosphoserine, anti-phosphotyrosine, and anti-phosphothreonine antibodies raised in rabbits were procured from Invitrogen (Grand Island, NY, USA). Amersham ECL rabbit IgG horseradish peroxidase-linked secondary antibody, ECL-Plus western blotting detection reagents and protein A/G beads were obtained from GE Healthcare (Pittsburgh, PA, USA). Anti-malate dehydrogenase (cytosolic) and anti-lactate dehydrogenase antibodies were purchased from Santa Cruz Biotechnology (Dallas, TX, USA). Anti-glucose-6-phosphate dehydrogenase antibody was obtained from Cell Signaling Technology (Danvers, MA, USA).

Animals

The brains from NMRs used in this study, aged 2–24 years, were obtained from the colonies maintained by Dr Rochelle Buffenstein at the University of Texas Health Science Center, San Antonio. These well-characterized colonies (Buffenstein 2005) were housed in fabricated burrow systems with climate conditions that mimicked their natural habitat (30°C and 30–50% relative humidity). Their diet consisted of fresh fruits and vegetables, provided *ad libitum*,

and supplemented with a high protein and vitamin enriched feed (Pronutro, South Africa). NMRs were anesthetized with isofluorane and then killed via cardiac exsanguination. Brains were immediately harvested and flash frozen in liquid nitrogen. All animal procedures were approved by the Institutional Animal Care and Use Committee at the University of Texas Health Science Center at San Antonio, TX. The experimental groups of animals consisted of both male and female breeding and non-breeding adults. For the four age groups, n = 5–9 individual brains.

Sample preparation

NMR brains were thawed and individual homogenates were prepared using a Wheaton glass homogenizer (~ 40 passes) with ice-cold isolation buffer [0.32 M sucrose, 2 mM EDTA, 2 mM EGTA, 20 mM HEPES, 0.2 μg/mL phenylmethylsulfonyl fluoride, 4 μg/mL leupeptin, 4 μg/mL pepstatin, 5 μg/mL aprotinin and 10 μg/mL phosphatase inhibitor cocktail 2]. Homogenates were vortexed on ice and sonicated for 10 s at 20% power with a Fisher 550 Sonic Dismembrator (Pittsburgh, PA, USA). Protein concentrations of the homogenates were determined by the Pierce bicinchoninic acid method (Smith *et al.* 1985).

Two-dimensional polyacrylamide gel electrophoresis

Isoelectric focusing

Two-dimensional polyacrylamide gel electrophoresis experiments were conducted as described previously (Sultana *et al.* 2007). Briefly, 200 μg of each homogenate was shaken for 2 h at 22°C in 200 μL of rehydration buffer [8 M urea, 2.0% (w/v) CHAPS, 2 M thiourea, 50 mM DTT, 0.2% biolytes, 0.01% bromophenol blue]. Samples were then sonicated for 10 s and dispensed into wells for application to 11 cm pH 3-10 ReadyStrip IPG strips for isoelectric separation of the proteins. Strips were actively rehydrated at 20°C for 18 h at 50 V using a Bio-Rad Protean Isoelectric focusing (IEF) Cell. Isoelectrical focusing continued at a constant temperature of 20°C beginning at 300 V for 2 h, 500 V for 2 h, 1000 V for 2 h, 8000 V for 8 h, and finishing at 8000 V for 10 h. IPG strips were then immediately stored at −80°C.

SDS–PAGE

IEF strips were thawed and then equilibrated for 10 min in the dark with 4 mL of equilibration buffer A [50 mM Tris–HCl, pH 6.8, 6 M urea, 1% (w/v) sodium dodecyl sulfate (SDS), 30% v/v glycerol, 0.5% DTT]. Strips were then re-equilibrated for 10 min in the dark with 4 mL of equilibration buffer B [50 mM Tris–HCl, pH 6.8, 6 M urea, 1% (w/v) SDS, 30% v/v glycerol, 4.5% IA]. The IEF strips were rinsed in a 1X dilution of TGS running buffer and placed into Criterion precast polyacrylamide gels (8–16% Tris–HCl, linear gradient), 1 IPG + 1 Well Comb, 11 cm. Precision Plus Protein All Blue molecular weight marker was added and the wells were overlaid with agarose gel. The gels were run at a constant voltage of 200 V for approximately 65 min at 22°C in 1X Tris/Glycine/SDS running buffer using a Criterion Cell vertical electrophoresis buffer tank.

SYPRO Ruby and Pro-Q Diamond staining

Gel staining to detect proteins and phosphoproteins was carried out according to manufacturer's directions and as previously described (Triplett *et al.* 2015). In brief, gels were fixed, stained with Pro-Q Diamond, scanned at 580 nm using a Bio-Rad ChemiDoc XRS+ imaging system (Bio-Rad), stained with Sypro Ruby, and then scanned again at 450 nm. Gels were stored in deionized water at 4°C until extraction of the protein spots.

Image analysis

Expression proteomics

Spot intensities from SYPRO Ruby-stained 2D-gel images of NMR samples were quantified by densitometry according to the total spot density using PDQuest 2-D Analysis Software (Bio-Rad). Intensities of individual spots were normalized to the total density of the gel. Spot densities of the three older age groups (4–6 year-olds, 7–12 year-olds, and 15–24 year-olds) were independently compared to the spot densities from the earliest age group (2–3 year-olds) using a Student's two-tailed t-test and a Mann–Whitney U statistical test, both at 95% confidence (i.e., $p < 0.05$). Only spots with a significant difference in both tests were considered for in-gel trypsin digestion and subsequent identification.

Phosphoproteomics

Protein spots from Pro-Q Diamond-stained 2D-gel images of the NMR samples were quantified and matched together in the same manner as the SYPRO Ruby-stained gels. Next, the master gel from the Sypro Ruby matching and Pro-Q Diamond matching were used for a high match analysis. The PDQuest software provided numerical data based on the intensity of each protein spot. The phosphoprotein spot densities were then normalized to the Sypro Ruby spot densities and the resultant normalized phosphoprotein spot densities in the three older age groups were independently compared to the earliest age group using a Student's two-tailed t-test and a Mann–Whitney U statistical test. Only spots that were significant ($p < 0.05$) in both tests were considered for in-gel trypsin digestion and subsequent identification.

In-gel trypsin digestion/peptide extraction

Significant spots were excised from 2D-gels and transferred to individual Eppendorf microcentrifuge tubes for trypsin digestion as described previously (Thongboonkerd *et al.* 2002). Briefly, gels were washed with 0.1 M ammonium bicarbonate (NH_4HCO_3) for 15 min, followed by incubation with acetonitrile (ACN) for 15 min. The solution was removed and gel plugs were allowed to dry under a flow hood. Next, the gel plugs were incubated in 20 mM DTT in 0.1 M NH_4HCO_3 for 45 min at 56°C. The DTT/NH_4HCO_3 solution was removed and 0.05 M IA in 0.1 M NH_4HCO_3 was added and allowed to incubate at 22°C for 15 min. The IA solution was removed and 150 μL of 0.05 M NH_4HCO_3 was added and incubated for 15 min at 22°C. Next, 200 μL of ACN was added and allowed to incubate for 15 min at 22°C. The solution was then removed and the gel plugs were allowed to dry under a flow hood. Then, 10 μL of modified trypsin solution in 0.05 M NH_4HCO_3 was added and incubated with shaking overnight at 37°C. Salts and contaminants were removed from the tryptic peptide solutions using C_{18} ZipTips. Samples were stored at −80°C until MS/MS analysis.

NanoLC-MS with data-dependent scan

Tryptic peptide solutions were reconstituted in 10 μL 5% ACN/0.1% formic acid (FA). MS/MS analysis was performed by a

nanoAcquity (Waters, Milford, MA, USA)-LTQ Orbitrap XL (Thermo Scientific, San Jose, CA, USA) system using a data-dependent scan mode. A capillary column packed in-house (0.1 × 130 mm column packed with 3.6 μm, 200Å XB-C18) was used. For separation, a gradient with 0.1% FA and ACN/0.1% FA at 200 nL/min was used. The MS spectra were obtained by the orbitrap at 30 000 resolution. The MS/MS spectra of the six most intense ions in MS scan were acquired by the orbitrap at 7500 resolution. Using the Swiss-Prot database by SEQUEST (Proteome Discoverer v1.4; Thermo Scientific), data files of each sample were interrogated. For protein identification, at least two high-confidence peptide matches were used (false discovery rate < 1%). Proteins that were matched with the same peptides were reported as one protein group. Data from the MS/MS analysis were initially verified by comparing the expected molecular weight and isoelectric point of the identified protein to that of the extracted plug from the 2-D gel.

Immunoprecipitation and western blotting validations

Immunoprecipitation

Whole brain homogenates (250 μg) were suspended in 500 μL immunoprecipitation (IP) buffer [0.05% NP-40, leupeptin 4 μg/mL, pepstatin 4 μg/mL, aproprotin 5 μg/mL, phosphatase inhibitor cocktail 10 μg/mL] in a phosphate buffer solution, pH 8 [8 M NaCl, 0.2 M KCl, 1.44 M Na_2HPO_4, 0.24 M KH_2PO_4]. The samples were then precleared by incubation with Protein A/G – agarose beads for 1.5 h at 4°C and then incubated overnight with anti-malate dehydrogenase antibody (1 : 50 dilution) at 4°C. Samples were once again incubated with Protein A/G – agarose beads for 1.5 h at 4°C and then washed 5 times with IP buffer. The beads were preserved for a one-dimensional polyacrylamide gel electrophoresis experiment.

One-dimensional polyacrylamide gel electrophoresis

Whole brain homogenized protein extracts (50 μg) or beads from IP experiments were suspended in 4X sample loading buffer [0.5 M Tris, pH 6.8, 40% glycerol, 8% SDS, 20% β-mercaptoethanol, 0.01% Bromophenol Blue] diluted to 1X with distilled water. Samples were then heated at 95°C for 5 min, cooled on ice, and loaded into a Criterion precast (4–12% Bis-Tris) polyacrylamide 18 well gel. Gels were placed in a Criterion Cell vertical electrophoresis buffer tank filled with XT MOPS running buffer and run at 80 V for 15 min and then at 120 V for approximately 100 min.

1D-western blotting

1D-gels were transferred to nitrocellulose membranes (0.2 nm) using a Trans-Blot Turbo Blotting System (Bio-Rad). After the transfer, membranes were blocked with 3% bovine serum albumin in Wash Blot [150 mM NaCl, 3 mM NaH_2PO_4, 17 mM $NaHPO_4$ and 0.04% (v/v) Tween 20] at 22°C for 1.5 h. The membrane was incubated with a primary antibody (1 : 3000 dilution) in blocking solution with gentle rocking for 2 h at 22°C. After washing the blots three times for 5 min each, the blots were incubated with a horseradish peroxidase (1 : 5000) secondary antibody in Wash Blot at 22°C with gentle rocking. The membranes were washed three times in Wash Blot (10 min each) and developed chemiluminescently using Clarity Western ECL substrate. After developing in the dark for 5 min at 22°C, membranes were scanned using Bio-Rad ChemiDoc XRS+ imaging system and quantified using Image Lab software (Bio-Rad). Blots were then stripped with Re-Blot Plus Strong solution and washed three times with Wash Blot (5 min each). The membranes were then blocked in 3% bovine serum albumin for 1.5 h and incubated with an anti-tubulin antibody (1 : 5000) or with anti-phosphoserine, anti-phosphothreonine and anti-phosphotyrosine antibodies (1 : 6000) for 2 h. The membranes were washed, incubated with a secondary antibody, and developed as described above.

Statistical analysis

Initial statistical analyses of PDQuest data were performed conservatively using both a two-tailed Student's *t*-test and the Mann–Whitney U statistical test, comparing each age group independently to the earliest age group. A protein spot was considered statistically significant if $p < 0.05$ for both tests. A one-way ANOVA with *post hoc* Bonferroni *t*-test was used in determining significance ($p < 0.05$) between age groups for PDQuest data and western blot analysis. Fold-change values of protein spots were calculated by dividing the average, normalized spot intensities of the gels of the older age group by the average, normalized spot intensities of the gels of the younger age group in the comparison. Spot extraction and MS/MS analysis was conducted only for spots with a 40% fold change or greater in normalized spot density. Identifications of proteins acquired with the SEQUEST search algorithm were considered to be statistically significant if $p < 0.01$. All data are presented as mean±SEM.

Results

To evaluate age-related protein changes in the brain, the NMR were divided into four age groups: 2–3 year-olds (age group 1; young), 4–6 year-olds (age group 2; intermediate), 7–12 year-olds (age group 3; old) and 15–24 year-olds (age group 4; oldest). The average protein spot intensities from each age cohort were compared to determine significant differentially expressed and phosphorylated proteins. Figure 1(a)–(d) shows representative examples obtained from SYPRO Ruby-stained 2-D gel images of the isolated proteins from these four age groups with significant differentially expressed proteins labeled. Figure 2(a)–(d) shows characteristic 2-D gels of the isolated protein spots stained with Pro-Q Diamond showing significantly altered phosphorylation states identified in each age group. PDQuest and MS/MS analyses of all the significant proteins found 13 metabolic proteins whose expression and/or phosphorylation states were significantly altered in NMR brains with age. These results are summarized in Table 1. Other information provided in the table includes: the PDQuest spot number,

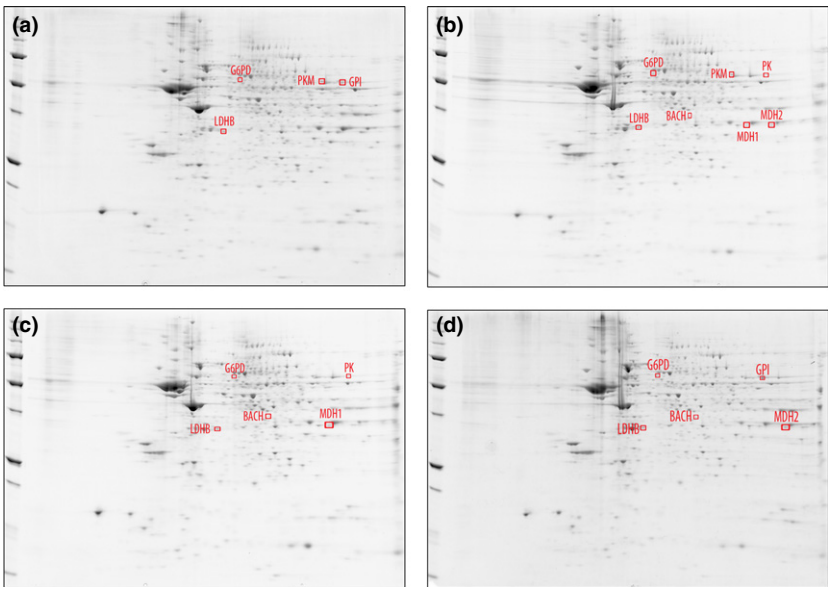

Fig. 1 Representative Sypro Ruby-stained 2-D gel images of isolated proteins from the brains of naked mole-rats (NMRs), aged 2–3 years (a), 4–6 years (b), 7–12 years (c), and 15–24 years (d). Proteins whose expression was statistically significantly altered in the particular age group are labeled in the images ($p < 0.05$).

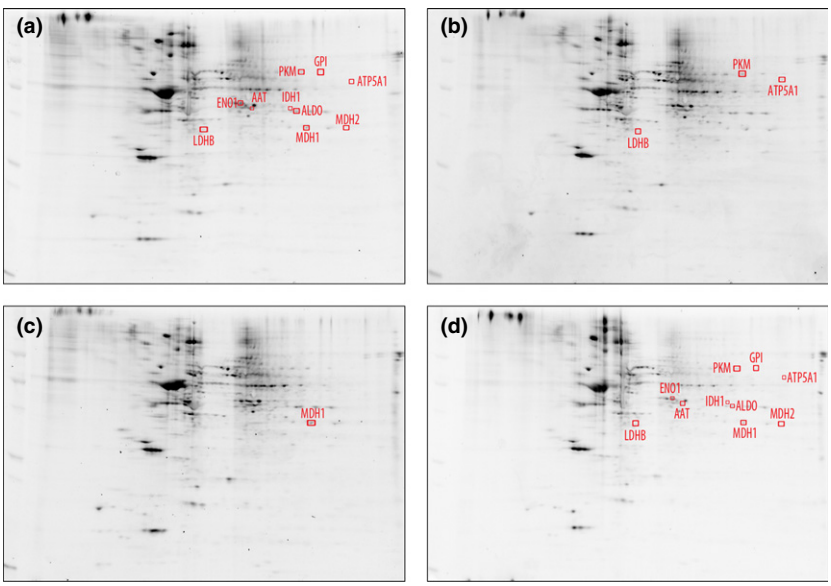

Fig. 2 Representative Pro-Q Diamond-stained 2-D gel images of isolated proteins from the brains of naked mole-rats (NMRs), aged 2–3 years (a), 4–6 years (b), 7–12 years (c), and 15–24 years (d). Proteins with statistically significantly altered phosphorylation states in the particular age group are labeled in the images ($p < 0.05$).

the SwissProt accession number, percentage of the protein sequence covered by matching peptides, the number of peptide sequences identified by the MS/MS analyses, the confidence score of the protein, the expected molecular weight and isoelectric point of the identified protein, the age groups compared with the corresponding *p*-values, and fold-change levels of expression and phosphorylation obtained from the PDQuest analyses. Two or more peptide sequences were used in the identification of all proteins; and the identified protein spots were visually compared against the expected molecular weights and isoelectric points to further ensure correct protein identification. Further details of the MS/MS analyses, including the amino acid sequence of the identified peptides are listed in Table S1. The 13 metabolic proteins found to have differential expression and/or phosphorylation states in one or more age groups were as follows: pyruvate kinase, pyruvate kinase M (PKM); glucose-6-phosphate 1 dehydrogenase; glucose-6-phosphate isomerase (GPI); malate dehydrogenase (both cytosolic and mitochondrial); L-lactate dehydrogenase B chain; cytosolic acyl-CoA thioester hydrolase; fructose-bisphosphate aldolase (ALDO); alpha enolase; cytosolic isocitrate dehydrogenase; aspartate aminotransferase; and ATP synthase subunit alpha (isoform 2).

To validate the identification of these proteins, IP and western blot validation experiments were undertaken. Fig-

Table 1 PDQuest and MS/MS results of NMR metabolic brain proteins with significant altered expression and/or phosphorylation states as a function of age

Spot	Protein identified	Accession #	Coverage (%)	No. of peptides	Score	MW (kDa)	pI	Age Groups compared	*p*-Value expression	Fold-change expression	*p*-Value phosphorylation	Fold-change phosphorylation
3309	L-lactate dehydrogenase, b chain	P07195	26.35	8	40.30	36.6	6.05	4 vs. 2	0.0336	2.24	0.0221	0.0132
								4 vs. 3	0.0133	2.70	–	–
4604	Glucose-6-P dehydrogenase	P11413	11.26	6	22.99	59.2	6.84	4 vs. 2	0.0337	2.70	–	–
								4 vs. 3	0.0219	2.99	–	–
5311	Cytosolic acyl-CoA thioester hydrolase	K7EKP8	15.71	4	16.81	30.8	6.99	3 vs. 1	0.0378	19.6	–	–
								4 vs. 3	0.0489	0.211	–	–
5503	Alpha enolase	P06733	23.04	8	44.68	47.1	7.39	4 vs. 1	–	–	0.0396	0.320
6402	Aspartate aminotransferase, cytoplasmic	P17174	9.20	5	26.85	46.2	7.01	4 vs. 1	–	–	0.0378	38.9
7312	Fructose-bis-P aldolase	H3BQN4	11.63	4	24.83	39.3	8.40	4 vs. 1	–	–	0.0476	0.182
7313	Malate dehydrogenase, cytoplasmic	B8ZZ51	18.34	3	19.11	18.7	5.94	3 vs. 1	0.0339	5.03	0.0129	0.0770
								4 vs. 1	–	–	0.0221	0.177
7402	Isocitrate dehydrogenase, cytoplasmic	O75874	12.56	5	22.41	46.6	7.01	4 vs. 1	–	–	0.0360	0.232
7604	Pyruvate kinase M	P14618	22.60	12	56.90	57.9	7.84	2 vs. 1	0.0460	4.45	0.0380	0.0152
								4 vs. 1	–	–	0.0429	0.167
7609	Glucose-6-P isomerase	K7EQ48	6.02	2	16.02	53.4	8.68	4 vs. 1	–	–	0.0331	0.251
								4 vs. 2	0.0184	3.93	–	–
8304	Malate dehydrogenase, mitochondrial	P40926	39.05	10	58.70	35.5	8.68	4 vs. 1	0.0436	4.53	0.0456	0.106
8604	Pyruvate kinase	H3BTN5	11.34	6	27.52	53.0	6.84	3 vs. 1	0.0476	83.7	–	–
8607	ATP synthase subunit alpha, isoform 2	P25705-2	30.82	13	96.61	56.5	8.24	4 vs. 1	–	–	0.0198	0.171
								4 vs. 2	–	–	0.0317	0.158

ure 3(a)–(d) shows the western blot images using tubulin as a loading control verifying the age-related changes in expression of lactate dehydrogenase (LDH) and glucose-6-phosphate dehydrogenase (G6PD) with corresponding bar graph representations of the data. The results of the western blot analyses of the expression of LDH confirmed a significant increase in the oldest age group as compared to the intermediate age group ($p = 0.0003$) and to the old age group ($p = 0.0003$). In addition, the western blot analysis also showed a statistically significant increase ($p = 0.024$) in the oldest age group as compared to the youngest age group. Western blot analysis of G6PD confirmed a significant increase in the level of G6PD in the brains of the oldest age group as compared to the intermediate ($p = 0.0103$) and old age group ($p = 0.014$). Figure 4 shows the images from the IP experiments after probing with anti-phosphoserine, anti-phosphothreonine and anti-phosphotyrosine antibodies in which the immunoprecipitated protein, cytosolic malate dehydrogenase 1 (MDH1), was used as the loading control. The findings from this analysis confirmed a significant decrease in the phosphorylation of MDH1 in the NMR brain for the old age group ($p = 0.044$) and in the oldest age group ($p = 0.03$), both as compared to the youngest age group.

Discussion

Numerous alterations of metabolism are evident in a number of age-related diseases such as Alzheimer's, Huntington's and Parkinson's diseases, cancer, atherosclerosis, and type 2 diabetes mellitus, to name but a few (Berg *et al.* 2002; Kahn 2003; Hsu and Sabatini 2008; Cai *et al.* 2012; Butterfield *et al.* 2014). Many of these metabolic diseases directly impact upon brain function, for the brain is an organ with a high rate of metabolism, consuming up to 20% of total glucose and 30% of inspired oxygen to maintain neuronal resting potentials, propagate action potentials, release neurotransmitters, and other energy-requiring processes (Madsen *et al.* 1999). With age, energy metabolism in the brain undergoes a gradual decline and the efficacy of these essential brain functions correspondingly diminishes, thereby contributing to age-related cognitive deficits (Petit-Taboué *et al.* 1998; Poon *et al.* 2006; Navarro and Boveris 2007; Swerdlow 2007). Therefore, examining the age-related changes in metabolic proteins in the brains of the NMR and understanding the mechanisms that contribute to the resistance of senescence-related diseases in NMRs conceivably may provide crucial clues to metabolic mechanisms that promote successful aging and increased health span.

Levels of pyruvate kinase (PK) were increased in the old NMR age group as compared to the youngest age group, whereas normally in rodents, this ATP generating enzyme decreases with age (Chainy and Kanungo 1978). Furthermore, the expression of a specific isoform of PK, PKM, was higher in the intermediate age group relative to the youngest NMR group studied, and the phosphorylation state was decreased in both the intermediate and oldest age group in relation to the youngest. Moreover, dephosphorylation of PKM has been shown to increase activity of PKM (Anastasiou *et al.* 2012). Increased PKM activity reportedly promotes anti-tumor activity by inhibiting tumor cell growth

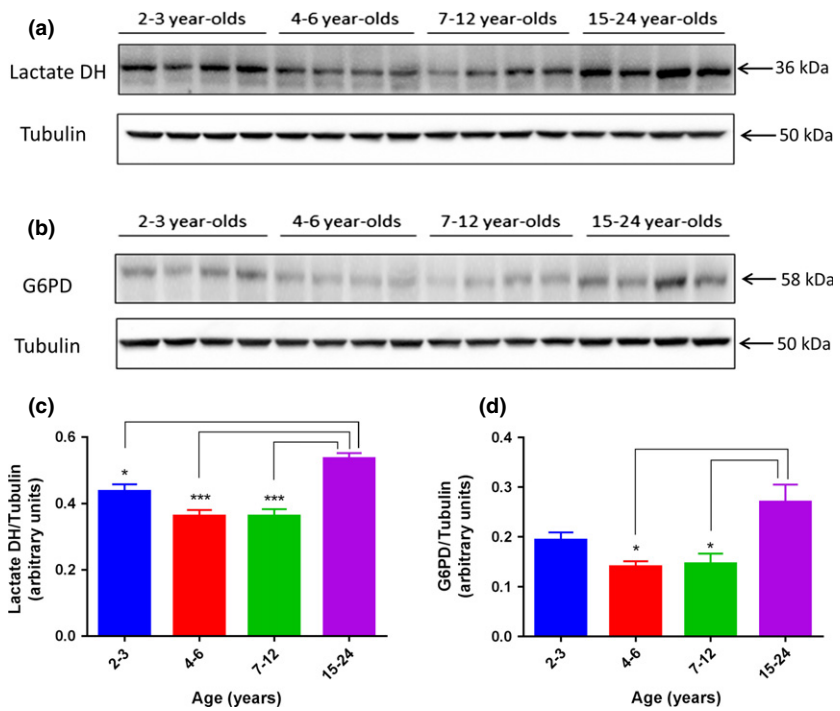

Fig. 3 Western blot and corresponding bar graph representations from the validation experiments of the changes in the expression of lactate dehydrogenase (a and c) and glucose-6-phosphate dehydrogenase (b and d) in the brains of naked mole-rats (NMRs) ($n = 4$ for each age group, $*p < 0.05$, $***p < 0.001$). Immunoreactivity with specific antibodies was detected by chemiluminescence.

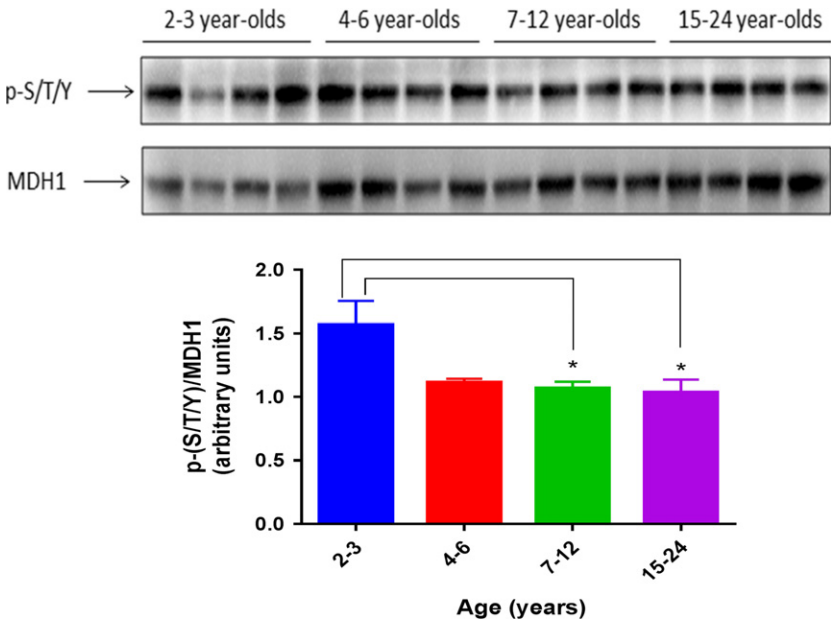

Fig. 4 Western blot and corresponding bar graph representation from immunochemistry experiments of the validation of the significant decrease in the phosphorylation of cytosolic malate dehydrogenase in the brains of naked mole-rats (NMRs) ($n = 4$ for each age group, $*p < 0.05$). Immunoreactivity of anti-MDH1 antibody was detected by chemiluminescence.

(Stetak *et al.* 2007; Anastasiou *et al.* 2012). Therefore, it is conceivable that the decreased phosphorylation state of PKM likely increases PKM activity in older NMRs and may contribute to their cancer resistance. Furthermore, the increased expression of PK in the old age cohort as well as the decreased phosphorylation of PKM in the oldest group, are mechanisms that conceivably contribute to sustaining the required energy demand during old age to maintain efficient cellular functioning.

Cytosolic acyl-CoA thioester hydrolase, also known as brain acyl-CoA hydrolase (BACH), catalyzes the cleavage of acyl-CoA producing a fatty acid and coenzyme A (CoA-SH), thereby modulating many cellular processes. Activity of BACH is higher in the brain than in any other organ, and acyl-CoA, fatty acids and CoA-SH are involved in cellular signaling, β-oxidation, inflammation, ion fluxes, protein and vesicle trafficking, allosteric regulation of enzymes, gene expression, lipid synthesis, and energy metabolism and regulation (Hunt and Alexson 2002; Yamada *et al.* 2002; Yamada 2005). BACH's role in regulating lipid metabolism may be a crucial factor affecting the aging rate by providing cell and membrane stability (Hulbert *et al.* 2007). The brain is rich in lipid content, and BACH is reportedly essential in the prevention of neurotoxicity by the dysregulation of neuronal fatty acid metabolism (Ellis *et al.* 2013). Analysis of BACH levels showed a significant increase from young to old NMR, which then significantly decreased in brains of the oldest age group. Normally, in rodents such as rats, BACH levels as well as metabolism of acyl-CoA declines with age to a steady level (Smith and Sun 1981). In contrast, in the NMR, levels of BACH increase with age, peaking in the old age group. In addition, it is noteworthy that although BACH levels drop in the elderly NMR population, the level is still higher than the BACH levels of the youngest cohort. Therefore, it is conceivable that these increased levels of BACH promote increased cellular integrity and regulation of β-oxidation that provides the membrane stability and energy regulation necessary for a healthy cellular environment.

Glucose-6-phosphate isomerase (a.k.a. neuroleukin; autocrine motility factor) is a pleiotropic protein performing different functions inside the cell and in the extracellular space. In the cytoplasm, GPI catalyzes the second step in glycolysis, regulates gp78-dependent mitochondrial fission and mitophagy (Fu *et al.* 2013; Shankar *et al.* 2013), and is reported to protect against ER stress and apoptosis by regulation of ER calcium release (Fu *et al.* 2011). Outside the cell, GPI acts as a neurotropic factor for spinal and sensory neurons, contributing to maintenance of neuronal integrity (Haga *et al.* 2000). A decrease in phosphorylation of GPI has been reported to lead to an increase in activity (Yanagawa *et al.* 2005). Hence, the increased levels of GPI relative to the earliest age group and the decreased phosphorylation levels in the oldest age cohort as compared to the intermediate, demonstrate a potential neuroprotective mechanism that may contribute to the NMR's sustained life span and health span.

Two additional glycolytic enzymes were identified as being significantly altered in the NMR brain: fructose-bisphosphate ALDO and alpha enolase (ENO1). ALDO is a pleiotropic protein that not only catalyzes a key reaction in glycolysis but is also involved in endocytosis, assembly and regulation of vacuolar H+-ATPase proton pump, mRNA stability, regulation of glucose transport, and assembly of the actin cytoskeleton (Kao *et al.* 1999; Lundmark and Carlsson 2004; Canete-Soler *et al.* 2005; Lu *et al.* 2007). In this study, the phosphorylation state of ALDO was decreased in the

oldest age group as compared to the youngest. Considering the aforementioned roles of ALDO, it is tempting to speculate that an increase in ALDO activity via a decreased phosphorylation state may contribute to salubrious longevity in the NMR; yet, the functional effects of ALDO phosphorylation have yet to be elucidated. However, as ALDOC was previously reported to have an increase in phosphorylation of 4.1-fold in the hippocampus of Alzheimer's disease (AD) brain (Di Domenico *et al.* 2011) and NMR brains have very high levels of both beta amyloid (Edrey *et al.* 2013) and phosphorylated tau (Orr *et al.* 2014) (pathological hallmarks of AD), elevated ALDO phosphorylation in AD may be pathological and the decrease with age in the phosphorylation level of this protein in NMR brains may reflect a potential mechanism used by NMRs in an attempt to better cope with these potentially toxic proteins.

ENO1 is a pleiotropic glycolytic enzyme that also acts as a neurotrophic factor, a hypoxic stress protein, a transcription factor in tumor formation and metastasis, a plasminogen binding protein in human diseases, an activator of plasminogen, and others (Butterfield and Lange 2009; Sedoris *et al.* 2010; Yamada *et al.* 2014). Previously, we have shown ENO1 to be oxidatively modified and differentially expressed in several age-related neurodegenerative disorders (Castegna *et al.* 2002; Perluigi *et al.* 2005a,b; Poon *et al.* 2005). Furthermore, ENO1 was shown to have an increased phosphorylation by 2.5-fold in the AD brain (Di Domenico *et al.* 2011). Conversely, in this study, the phosphorylation of ENO1 was shown to be decreased by 68% in the oldest NMR age group relative to the youngest age group. Therefore, we speculate that decreased phosphorylation of ENO1 may be a contributing factor to increased life span and health span in the NMR.

Lactate dehydrogenase B chain (LDHB) is one of five LDH isoforms that catalyze the interconversion between pyruvate and lactate. LDHB activity preferentially favors the oxidation of lactate to pyruvate, generating energy (Newington *et al.* 2013). Moreover, levels of LDH are reportedly increased in senescent human fibroblasts (Zwerschke *et al.* 2003), and high amounts of lactate in brain, as a consequence of decreased LDHB, have been suggested to be an aging hallmark (Ross *et al.* 2010). Therefore, given that NMRs live in a hypoxic environment in the wild, the increase in LDHB levels in the oldest NMR cohort as compared to both the intermediate and old cohorts conceivably may be a neuroprotective mechanism to increase energy output.

Malate dehydrogenase 2 (MDH2) is a mitochondrial TCA enzyme that catalyzes the conversion of oxaloacetate to malate producing NADH. When compared with the youngest NMR, MDH2 levels were significantly increased in the oldest age group with a decrease in phosphorylation state. Phosphorylation of MDH has been reported to decrease its activity (Minard and McAlister-Henn 1994), suggesting that aged NMR brains may be effectively regulating the high levels of MDH2 through inhibitory phosphorylation and thereby maintain a physiologic level of activity. Malate dehydrogenase in the cytosol (MDH1) is a metabolic protein of the malate-aspartate shuttle that is necessary in the transference of reducing equivalents of NADH into the mitochondria for the use by complex I of the electron transport chain. MDH1 levels were greater in the old age group with a decrease in phosphorylation in the two oldest age groups, all as compared to the youngest cohort. An increased level of this key enzyme would result in increased mitochondrial ATP synthesis. Consequently, the elevated levels of MDH1 and MDH2, along with their decreased phosphorylation states in brains from the oldest group of NMR are consistent with an increase in energy metabolism that may contribute to NMR health and longevity. Congruous with our results, MDH1 is reportedly decreased in aged human fibroblasts (Lee *et al.* 2012); and, in MDH1 knockdown cells, sirtuin 1 deacetylase, a regulator of cellular senescence, is decreased, suggesting that MDH1 plays a role in the regulation of senescence (Lee *et al.* 2012) and could contribute to increased life span of these rodents.

Aspartate aminotransferase is another malate-aspartate shuttle enzyme that also plays a key role in the biosynthesis of purines, pyrimidines, amino acids, and their derivatives (Wrenger *et al.* 2012), as well as the reversible transamination of α-ketoglutarate (α-KG) to glutamate. These steps are essential for the production of DNA and RNA, increased synthesis of ATP, and the formation of the major excitatory neurotransmitter, glutamate. The precise role of the altered phosphorylation state is unclear, but it was increased in the brain of the oldest NMR group relative to the youngest age group; and this increase may be consistent with the need for elevation of glutamate in extended aging and increased neuroplasticity (Segovia *et al.* 2001; Mattson 2008).

Cytoplasmic isocitrate dehydrogenase (IDH1) catalyzes the oxidative decarboxylation of isocitrate that produces α-KG generating NADPH to aid in defense against reactive oxygen species (Bleeker *et al.* 2010). In aged cells, IDH activity is reported to be markedly decreased (Samokhvalov *et al.* 2004). In contrast, in the brain of NMR, the phosphorylation state of IDH1 was significantly decreased in the oldest age group, relative to the youngest age group, and a decreased phosphorylation state has been shown to increase the activity of the enzyme (LaPorte 1993). This is consistent with the notion that decreased phosphorylation of IDH1 contributes to the increased life span of NMRs.

Glucose-6-phosphate 1 dehydrogenase (G6PD) shunts glucose-6-phosphate from the glycolytic pathway to the pentose phosphate pathway, also producing NADPH as well as pentose phosphates for fatty acid and nucleic acid synthesis. G6PD levels were higher in the oldest age group as compared to both the intermediate and old age groups. Therefore, the up-regulation of G6PD may promote a reduced cellular state to encourage a neuroprotective environment.

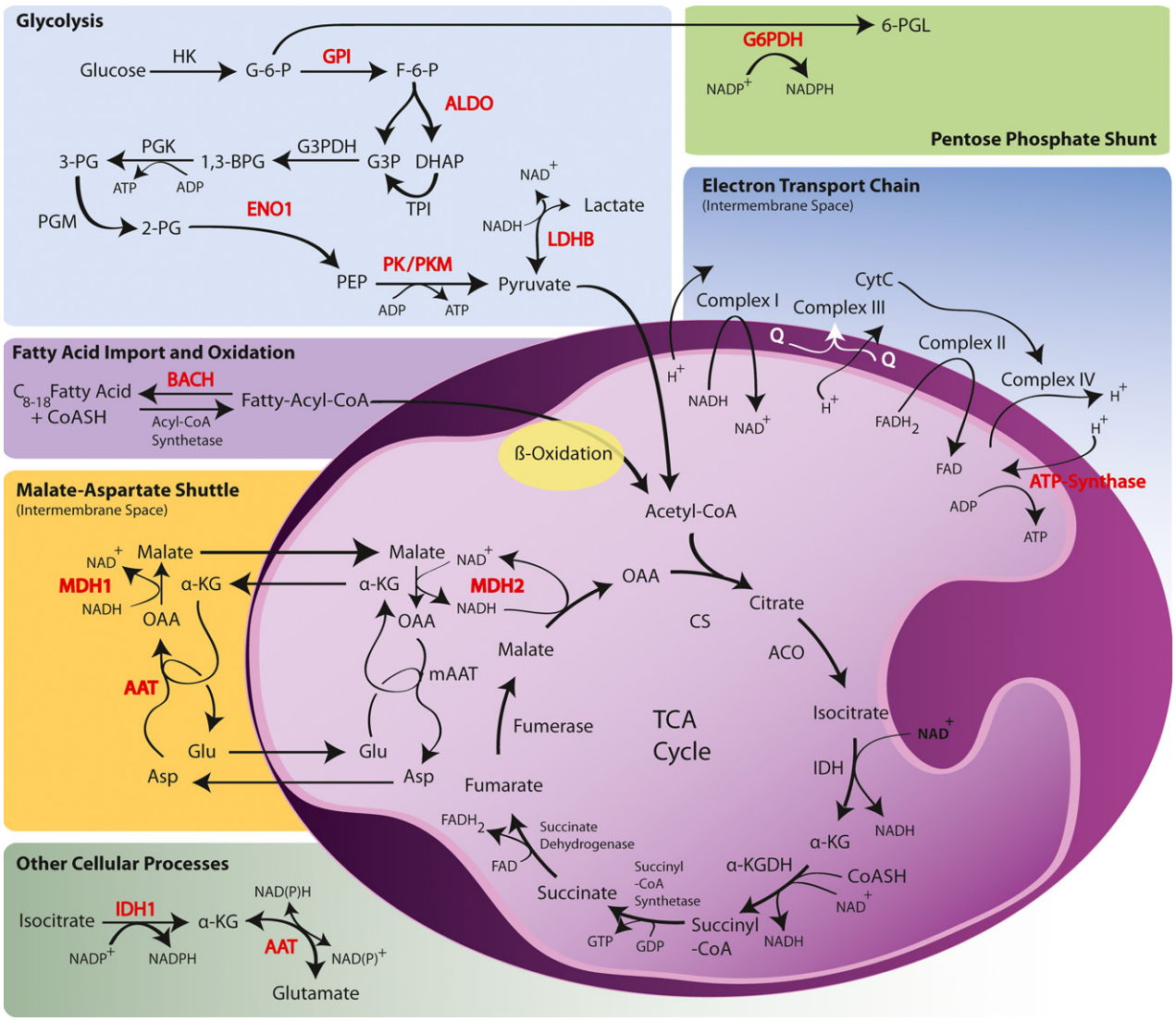

Fig. 5 Summary schematic diagram of expression proteomics and phosphoproteomics profiles of metabolic protein changes in the brain of the naked mole-rat (NMR) as a function of age. Proteins with altered levels and/or phosphorylation states are highlighted in red. See Discussion section for more details.

ATP synthase subunit alpha (ATP5A1) is among the catalytic subunits of complex V of the electron transport chain. With age, ATP production declines. However, in the oldest NMR cohort, ATP5A1 (isoform 2) was found to have decreased inhibitory phosphorylation relative to both the young and intermediate age groups. Phosphorylation of ATP5A1 has been reported to decrease activity as a consequence of decreased binding affinity to ATP (Alzamora *et al.* 2010). Therefore, our results are consistent with the notion that as NMRs age, ATP production is increased, fueling key cellular processes.

Because this study involved both male and female and both breeding and non-breeding animals, a potential caveat for these results may be the contribution of breeding status, which could possibly introduce sample variation because of hormonal differences (Margulis *et al.* 1995). Future studies, with many more animals, will be necessary to estimate the contribution of breeding status to the results obtained. Furthermore, it is tempting to speculate that the significant differences found between the youngest cohort and the other ages may represent an immature brain in its final steps of development. Studies dedicated to understanding and characterizing NMR brain development are needed to clarify this potential caveat common among this and many prior NMR studies.

In summary, this study has identified significant alterations in protein levels and phosphorylation states of key metabolic proteins. The metabolic pathways in which these proteins are involved are illustrated in Fig. 5. Furthermore, many of these proteins are pleiotropic, having many other interesting

functions that may contribute to the exceptional longevity and disease resistance of the NMR. The results obtained using proteomics and phosphoproteomics have revealed important potential mechanisms for increased life span and increased health span of NMRs. An improved understanding of mechanisms that facilitate extended life span and health span in the NMR may conceivably afford insights into the prevention of age-related diseases in humans, potentially leading to therapies that may slow the onset and progression of the aging process.

Acknowledgments and conflict of interest disclosure

These studies were supported in part by funds from the University of Kentucky Research Challenge Trust Fund. The authors have no conflicts of interest to declare.

All experiments were conducted in compliance with the ARRIVE guidelines.

Supporting information

Additional supporting information may be found in the online version of this article at the publisher's web-site:

Table S1. Additional data from the MS/MS identification of the extracted gels spots to supplement those from Table 1 in the text and include: the amino acid sequence of the high-confidence-matched peptides, the number of peptide-spectrum matches (PSMs), the posterior error probability (PEP), the cross-correlation (XCorr) number, and the number of missed cleavages (from the trypsin digestion).

References

Ables G. P., Brown-Borg H. M., Buffenstein R. *et al.* (2014) The first international mini-symposium on methionine restriction and lifespan. *Front. Genet.* **5**, 122.

Alzamora R., Thali R. F., Gong F. *et al.* (2010) PKA regulates vacuolar H+-ATPase localization and activity via direct phosphorylation of the a subunit in kidney cells. *J. Biol. Chem.* **285**, 24676–24685.

Anastasiou D., Yu Y., Israelsen W. J. *et al.* (2012) Pyruvate kinase M2 activators promote tetramer formation and suppress tumorigenesis. *Nat. Chem. Biol.* **8**, 839–847.

Berg A. H., Combs T. P. and Scherer P. E. (2002) ACRP30/adiponectin: an adipokine regulating glucose and lipid metabolism. *Trends Endocrinol. Metab.* **13**, 84–89.

Bleeker F. E., Atai N. A., Lamba S. *et al.* (2010) The prognostic IDH1 (R132) mutation is associated with reduced NADP+-dependent IDH activity in glioblastoma. *Acta Neuropathol.* **119**, 487–494.

Bobeck B. (1969) Survival turnover and production of small rodents in beech forest. *Acta Theriol.* **18**, 403–434.

Buffenstein R. (2005) The naked mole-rat: a new long-living model for human aging research. *J. Gerontol. A Biol. Sci. Med. Sci.* **60**, 1369–1377.

Buffenstein R. (2008) Negligible senescence in the longest living rodent, the naked mole-rat: insights from a successfully aging species. *J. Comp. Physiol. B.* **178**, 439–445.

Buffenstein R., Nelson O. L. and Corbit K. C. (2014) Questioning the preclinical paradigm: natural, extreme biology as an alternative discovery platform. *Aging* **6**, 913–920.

Buffenstein R. and Yahav S. (1991a) The effect of diet on microfaunal population and function in the caecum of a subterranean naked mole-rat, Heterocephalus glaber. *Br. J. Nutr.* **65**, 249–258.

Buffenstein R. and Yahav S. (1991b) Is the naked mole-rat Hererocephalus glaber a poikilothermic or poorly thermoregulating endothermic mammal? *J. Therm. Biol* **16**, 227–232.

Butterfield D. A., Di Domenico F. and Barone E. (2014) Elevated risk of type 2 diabetes for development of Alzheimer disease: a key role for oxidative stress in brain. *Biochim. Biophys. Acta* **1842**, 1693–1706.

Butterfield D. A. and Lange M. L. (2009) Multifunctional roles of enolase in Alzheimer's disease brain: beyond altered glucose metabolism. *J. Neurochem.* **111**, 915–933.

Cai H., Cong W. N., Ji S., Rothman S., Maudsley S. and Martin B. (2012) Metabolic dysfunction in Alzheimer's disease and related neurodegenerative disorders. *Curr. Alzheimer Res.* **9**, 5–17.

Canete-Soler R., Reddy K. S., Tolan D. R. and Zhai J. (2005) Aldolases a and C are ribonucleolytic components of a neuronal complex that regulates the stability of the light-neurofilament mRNA. *J. Neurosci.* **25**, 4353–4364.

Castegna A., Aksenov M., Thongboonkerd V., Klein J. B., Pierce W. M., Booze R., Markesbery W. R. and Butterfield D. A. (2002) Proteomic identification of oxidatively modified proteins in Alzheimer's disease brain. Part II: dihydropyrimidinase-related protein 2, alpha-enolase and heat shock cognate 71. *J. Neurochem.* **82**, 1524–1532.

Chainy G. B. and Kanungo M. S. (1978) Induction and properties of pyruvate kinase of the cerebral hemisphere of rats of various ages. *J. Neurochem.* **30**, 419–427.

David J. H. M. and Jarvis J. U. M. (1985) Population Fluctuations, Reproduction and Survival in the Striped Fieldmouse Rhabdomys-Pumilio on the Cape Flats, South-Africa. *J. Zool.* **207**, 251–276.

Di Domenico F., Sultana R., Barone E., Perluigi M., Cini C., Mancuso C., Cai J., Pierce W. M. and Butterfield D. A. (2011) Quantitative proteomics analysis of phosphorylated proteins in the hippocampus of Alzheimer's disease subjects. *J. Proteomics.* **74**, 1091–1103.

Dumm C. L. A. G., Console G. M., Luna G. C., Dardenne M. and Goya R. G. (1995) Quantitative immunohistochemical changes in the endocrine pancreas of nonobese diabetic (Nod) mice. *Pancreas* **11**, 396–401.

Edrey Y. H., Hanes M., Pinto M., Mele J. and Buffenstein R. (2011) Successful aging and sustained good health in the naked mole rat: a long-lived mammalian model for biogerontology and biomedical research. *ILAR J.* **52**, 41–53.

Edrey Y. H., Medina D. X., Gaczynska M., Osmulski P. A., Oddo S., Caccamo A. and Buffenstein R. (2013) Amyloid beta and the longest-lived rodent: the naked mole-rat as a model for natural protection from Alzheimer's disease. *Neurobiol. Aging* **34**, 2352–2360.

Ellis J. M., Wong G. W. and Wolfgang M. J. (2013) Acyl coenzyme A thioesterase 7 regulates neuronal fatty acid metabolism to prevent neurotoxicity. *Mol. Cell. Biol.* **33**, 1869–1882.

Finch C. E. and Austad S. N. (2001) History and prospects: symposium on organisms with slow aging. *Exp. Gerontol.* **36**, 593–597.

Fu M., Li L., Albrecht T., Johnson J. D., Kojic L. D. and Nabi I. R. (2011) Autocrine motility factor/phosphoglucose isomerase regulates ER stress and cell death through control of ER calcium release. *Cell Death Differ.* **18**, 1057–1070.

Fu M., St-Pierre P., Shankar J., Wang P. T., Joshi B. and Nabi I. R. (2013) Regulation of mitophagy by the Gp78 E3 ubiquitin ligase. *Mol. Biol. Cell* **24**, 1153–1162.

Grimes K. M., Reddy A. K., Lindsey M. L. and Buffenstein R. (2014) And the beat goes on: maintained cardiovascular function during

aging in the longest-lived rodent, the naked mole-rat. *Am. J. Physiol. Heart Circ. Physiol.* **307**, H284–H291.

Guarente L. and Kenyon C. (2000) Genetic pathways that regulate ageing in model organisms. *Nature* **408**, 255–262.

Haga A., Niinaka Y. and Raz A. (2000) Phosphohexose isomerase/autocrine motility factor/neuroleukin/maturation factor is a multifunctional phosphoprotein. *Biochim. Biophys. Acta* **1480**, 235–244.

Hsu P. P. and Sabatini D. M. (2008) Cancer cell metabolism: warburg and beyond. *Cell* **134**, 703–707.

Hulbert A. J., Pamplona R., Buffenstein R. and Buttemer W. A. (2007) Life and death: metabolic rate, membrane composition, and life span of animals. *Physiol. Rev.* **87**, 1175–1213.

Hunt M. C. and Alexson S. E. (2002) The role Acyl-CoA thioesterases play in mediating intracellular lipid metabolism. *Prog. Lipid Res.* **41**, 99–130.

Jarvis J. U. (1981) Eusociality in a mammal: cooperative breeding in naked mole-rat colonies. *Science* **212**, 571–573.

Kahn S. E. (2003) The relative contributions of insulin resistance and beta-cell dysfunction to the pathophysiology of Type 2 diabetes. *Diabetologia* **46**, 3–19.

Kao A. W., Noda Y., Johnson J. H., Pessin J. E. and Saltiel A. R. (1999) Aldolase mediates the association of F-actin with the insulin-responsive glucose transporter GLUT4. *J. Biol. Chem.* **274**, 17742–17747.

Kramer B. and Buffenstein R. (2004) The pancreas of the naked mole-rat (Heterocephalus glaber): an ultrastructural and immunocytochemical study of the endocrine component of thermoneutral and cold acclimated animals. *Gen. Comp. Endocrinol.* **139**, 206–214.

LaPorte D. C. (1993) The isocitrate dehydrogenase phosphorylation cycle: regulation and enzymology. *J. Cell. Biochem.* **51**, 14–18.

Larson J. and Park T. J. (2009) Extreme hypoxia tolerance of naked mole-rat brain. *NeuroReport* **20**, 1634–1637.

Lee S. M., Dho S. H., Ju S. K., Maeng J. S., Kim J. Y. and Kwon K. S. (2012) Cytosolic malate dehydrogenase regulates senescence in human fibroblasts. *Biogerontology* **13**, 525–536.

Lewis K. N., Mele J., Hornsby P. J. and Buffenstein R. (2012) Stress resistance in the naked mole-rat: the bare essentials - a mini-review. *Gerontology* **58**, 453–462.

Lu M., Ammar D., Ives H., Albrecht F. and Gluck S. L. (2007) Physical interaction between aldolase and vacuolar H+-ATPase is essential for the assembly and activity of the proton pump. *J. Biol. Chem.* **282**, 24495–24503.

Lundmark R. and Carlsson S. R. (2004) Regulated membrane recruitment of dynamin-2 mediated by sorting nexin 9. *J. Biol. Chem.* **279**, 42694–42702.

Madsen P. L., Cruz N. F., Sokoloff L. and Dienel G. A. (1999) Cerebral oxygen/glucose ratio is low during sensory stimulation and rises above normal during recovery: excess glucose consumption during stimulation is not accounted for by lactate efflux from or accumulation in brain tissue. *J. Cereb. Blood Flow Metab.* **19**, 393–400.

Margulis S. W., Saltzman W. and Abbott D. H. (1995) Behavioral and hormonal changes in female naked mole-rats (Heterocephalus glaber) following removal of the breeding female from a colony. *Horm. Behav.* **29**, 227–247.

Mattson M. P. (2008) Glutamate and neurotrophic factors in neuronal plasticity and disease. *Ann. N. Y. Acad. Sci.* **1144**, 97–112.

Minard K. I. and McAlister-Henn L. (1994) Glucose-induced phosphorylation of the MDH2 isozyme of malate dehydrogenase in Saccharomyces cerevisiae. *Arch. Biochem. Biophys.* **315**, 302–309.

Navarro A. and Boveris A. (2007) The mitochondrial energy transduction system and the aging process. *Am. J. Physiol. Cell Physiol.* **292**, C670–C686.

Newington J. T., Harris R. A. and Cumming R. C. (2013) Reevaluating metabolism in Alzheimer's disease from the perspective of the astrocyte-neuron lactate shuttle model. *J. Neurodegenerative Dis.* **2013**, 13.

O'Connor T. P., Lee A., Jarvis J. U. and Buffenstein R. (2002) Prolonged longevity in naked mole-rats: age-related changes in metabolism, body composition and gastrointestinal function. *Comp. Biochem. Physiol. A Mol. Integr. Physiol.* **133**, 835–842.

Orr M. E., Salinas A., Buffenstein R. and Oddo S. (2014) Mammalian target of rapamycin hyperactivity mediates the detrimental effects of a high sucrose diet on Alzheimer's disease pathology. *Neurobiol. Aging* **35**, 1233–1242.

Perluigi M., Fai Poon H., Hensley K., Pierce W. M., Klein J. B., Calabrese V., De Marco C. and Butterfield D. A. (2005a) Proteomic analysis of 4-hydroxy-2-nonenal-modified proteins in G93A-SOD1 transgenic mice–a model of familial amyotrophic lateral sclerosis. *Free Radic. Biol. Med.* **38**, 960–968.

Perluigi M., Poon H. F., Maragos W., Pierce W. M., Klein J. B., Calabrese V., Cini C., De Marco C. and Butterfield D. A. (2005b) Proteomic analysis of protein expression and oxidative modification in r6/2 transgenic mice: a model of Huntington disease. *Mol. Cell Proteomics* **4**, 1849–1861.

Petit-Taboué M. C., Landeau B., Desson J. F., Desgranges B. and Baron J. C. (1998) Effects of healthy aging on the regional cerebral metabolic rate of glucose assessed with statistical parametric mapping. *NeuroImage* **7**, 176–184.

Poon H. F., Frasier M., Shreve N., Calabrese V., Wolozin B. and Butterfield D. A. (2005) Mitochondrial associated metabolic proteins are selectively oxidized in A30P alpha-synuclein transgenic mice–a model of familial Parkinson's disease. *Neurobiol. Dis.* **18**, 492–498.

Poon H. F., Shepherd H. M., Reed T. T., Calabrese V., Stella A. M., Pennisi G., Cai J., Pierce W. M., Klein J. B. and Butterfield D. A. (2006) Proteomics analysis provides insight into caloric restriction mediated oxidation and expression of brain proteins associated with age-related impaired cellular processes: mitochondrial dysfunction, glutamate dysregulation and impaired protein synthesis. *Neurobiol. Aging* **27**, 1020–1034.

Ross J. M., Oberg J., Brene S. *et al.* (2010) High brain lactate is a hallmark of aging and caused by a shift in the lactate dehydrogenase A/B ratio. *Proc. Natl Acad. Sci. USA* **107**, 20087–20092.

Samokhvalov V., Ignatov V. and Kondrashova M. (2004) Inhibition of Krebs cycle and activation of glyoxylate cycle in the course of chronological aging of Saccharomyces cerevisiae. Compensatory role of succinate oxidation. *Biochimie* **86**, 39–46.

Sedoris K. C., Thomas S. D. and Miller D. M. (2010) Hypoxia induces differential translation of enolase/MBP-1. *BMC Cancer* **10**, 157.

Segovia G., Porras A., Del Arco A. and Mora F. (2001) Glutamatergic neurotransmission in aging: a critical perspective. *Mech. Ageing Dev.* **122**, 1–29.

Shankar J., Kojic L. D., St-Pierre P., Wang P. T., Fu M., Joshi B. and Nabi I. R. (2013) Raft endocytosis of AMF regulates mitochondrial dynamics through Rac1 signaling and the Gp78 ubiquitin ligase. *J. Cell Sci.* **126**(Pt 15), 3295–3304.

Smith P. K., Krohn R. I., Hermanson G. T., Mallia A. K., Gartner F. H., Provenzano M. D., Fujimoto E. K., Goeke N. M., Olson B. J. and Klenk D. C. (1985) Measurement of protein using bicinchoninic acid. *Anal. Biochem.* **150**, 76–85.

Smith R. E. and Sun G. Y. (1981) Metabolism of acyl-CoA in the developing rat brain. *Dev. Neurosci.* **4**, 337–344.

Stetak A., Veress R., Ovadi J., Csermely P., Keri G. and Ullrich A. (2007) Nuclear translocation of the tumor marker pyruvate kinase M2 induces programmed cell death. *Cancer Res.* **67**, 1602–1608.

Sultana R., Boyd-Kimball D., Cai J., Pierce W. M., Klein J. B., Merchant M. and Butterfield D. A. (2007) Proteomics analysis of the Alzheimer's disease hippocampal proteome. *J. Alzheimers Dis.* **11**, 153–164.

Swerdlow R. H. (2007) Treating neurodegeneration by modifying mitochondria: potential solutions to a "complex" problem. *Antioxid. Redox Signal.* **9**, 1591–1603.

Thongboonkerd V., McLeish K. R., Arthur J. M. and Klein J. B. (2002) Proteomic analysis of normal human urinary proteins isolated by acetone precipitation or ultracentrifugation. *Kidney Int.* **62**, 1461–1469.

Tokuyama Y., Sturis J., DePaoli A. M., Takeda J., Stoffel M., Tang J., Sun X., Polonsky K. S. and Bell G. I. (1995) Evolution of beta-cell dysfunction in the male Zucker diabetic fatty rat. *Diabetes* **44**, 1447–1457.

Triplett J., Zhang Z., Sultana R., Cai J., Klein J. B., Bueler H. and Butterfield D. A. (2015) Quantitative expression proteomics and phosphoproteomics profile of brain from PINK1 knockout mice: insights into mechanisms of familial Parkinson disease. *J. Neurochem.* **133**, 750–765.

Wrenger C., Muller I. B., Silber A. M., Jordanova R., Lamzin V. S. and Groves M. R. (2012) Aspartate aminotransferase: bridging carbohydrate and energy metabolism in Plasmodium falciparum. *Curr. Drug Metab.* **13**, 332–336.

Yamada J. (2005) Long-chain acyl-CoA hydrolase in the brain. *Amino Acids* **28**, 273–278.

Yamada J., Kuramochi Y., Takagi M., Watanabe T. and Suga T. (2002) Human brain acyl-CoA hydrolase isoforms encoded by a single gene. *Biochem. Biophys. Res. Commun.* **299**, 49–56.

Yamada S., Marutsuka M., Inoue M., Zhang J., Abe S., Ishibashi K., Yamaguchi N. and Eto K. (2014) The interaction of the ErbB4 intracellular domain p80 with alpha-enolase in the nuclei is associated with the inhibition of the neuregulin1-dependent cell proliferation. *Int. J. Biochem. Mol. Biol.* **5**, 21–29.

Yanagawa T., Funasaka T., Tsutsumi S., Raz T., Tanaka N. and Raz A. (2005) Differential regulation of phosphoglucose isomerase/autocrine motility factor activities by protein kinase CK2 phosphorylation. *J. Biol. Chem.* **280**, 10419–10426.

Zwerschke W., Mazurek S., Stockl P., Hutter E., Eigenbrodt E. and Jansen-Durr P. (2003) Metabolic analysis of senescent human fibroblasts reveals a role for AMP in cellular senescence. *Biochem. J.* **376**(Pt 2), 403–411.